I-SOCIAL-DB: A Labeled Database of Images Collected from Websites and Social Media for Iris Recognition

Ruggero Donida Labati[a],*, Angelo Genovese[a], Vincenzo Piuri[a], Fabio Scotti[a] and Sarvesh Vishwakarma[b]

[a]Department of Computer Science, Università degli Studi di Milano, Milano, Italy
[b]Department of Computer Science, Indian Institute of Information Technology, Allahabad, India

ARTICLE INFO

ABSTRACT

People upload daily a huge number of portrait face pictures on websites and social media, which can be processed using biometric systems based on the face characteristics to perform an automatic recognition of the individuals. However, the performance of face recognition approaches can be limited by negative factors as aging, occlusions, rotations, and uncontrolled expressions. Nevertheless, the constantly increasing quality and resolution of the portrait pictures uploaded on websites and social media could permit to overcome these problems and improve the robustness of biometric recognition methods by enabling the analysis of additional traits, like the iris. To point the attention of the research community to the possible use of iris-based recognition techniques for images uploaded on websites and social media, we present a public image dataset called I-SOCIAL-DB (Iris Social Database). This dataset is composed of $3,286$ ocular regions, extracted from $1,643$ high-resolution face images of 400 individuals, collected from public websites. For each ocular region, a human expert extracted the coordinates of the circles approximating the inner and outer iris boundaries and performed a pixelwise segmentation of the iris contours, occlusions, and reflections. This dataset is the first collection of ocular images from public websites and social media, and one of the biggest collections of manually segmented ocular images in the literature. In this paper, we also present a qualitative analysis of the samples, a set of testing protocols and figures of merit, and benchmark results achieved using publicly available iris segmentation and recognition algorithms. We hope that this initiative can give a new test tool to the biometric research community, aiming to stimulate new studies in this challenging research field.

1. Introduction

Biometric technologies based on face recognition can be successfully used to identify a person using images collected from websites and social media, by comparing his or her face image against a large number of publicly available images. In this scenario, recent methods for face recognition can achieve satisfactory performance also with samples of limited size and resolution [21].

Nevertheless, the resolution and size of the images uploaded on websites and social media is constantly improving, thus possibly allowing the use of additional biometric characteristics to perform a more robust and accurate recognition. In fact, consumer-level digital cameras, as well as the cameras integrated in smartphones, are constantly adopting better sensors, lenses, and image processing algorithms. As an example, in 2019, Samsung presented the ISOCELL Bright HMX, a sensor able to acquire images of 108 megapixels [52]. Similarly, in the same year, Xiaomi introduced the Redmi Note 10, a smartphone integrating a camera with a resolution of 108 megapixels [58].

As a consequence of the higher resolution of the sensors, methods for mobile-based biometric recognition are being increasingly proposed in the literature [15, 34]. In this context, the face and ocular-based features are among the most relevant biometric characteristics that can be extracted from high-resolution images [47, 48, 49]. In particular, the iris texture is especially relevant for the following reasons [14].

- The iris can be considered as stable for almost the entire life. Automatic methods for searching individuals in sets of images uploaded on websites and social media could therefore become particularly useful investigative tools (e.g., for searching missing children).

- Iris recognition methods are usually characterized by a low False Match Rate (FMR). Therefore, recognition results confirming that two samples are from the same individual have a very high probability of being correct [9].

- The matching algorithms usually require less computational resources for iris-based biometric systems with respect to face recognition technologies. As an example, [33] reports that desktop computers can perform up to 25 million comparisons per second. Therefore, iris recognition systems could be applied to perform identifications in wider biometric databases.

- The iris characteristics can be used to perform biometric recognitions even in cases for which face recognition systems fail because of occlusions, rotations, unnatural expressions, or the presence of protective or surgical masks.

- The two iris textures present in the face image could be used to perform multibiometric recognitions, possibly

✉ ruggero.donida@unimi.it (R. Donida Labati)
🌐 www.di.unimi.it/donida (R. Donida Labati)
ORCID(s): 0000-0002-2636-086X (R. Donida Labati)

in conjunction with the face. In most of the cases, multimodal biometric systems permit to increase the accuracy and robustness of monomodal systems [51].

Despite the advantages of recognition methods based on the iris texture, the traditional iris acquisition procedure presents several constraints. In fact, most of the iris recognition systems use near-infrared illuminators and require the users to be highly cooperative by staying still at a close distance from the acquisition sensor, opening the eyes, and looking in a fixed direction [7]. Nevertheless, recent studies on iris recognition proved that it is possible to reduce such constraints and perform biometric recognitions by processing ocular images acquired in less-constrained conditions, for example by using images captured with smartphone cameras, in natural light illumination, at a distance, or on-the-move [3, 12, 16, 17, 18].

To enable the design of iris recognition methods using images captured in less-constrained conditions, researchers freely released public databases of ocular images acquired in scenarios characterized by limited acquisition constraints [13, 26, 41, 43, 49, 54, 56]. However, images collected from websites and social media have not been used for iris recognition until now.

Ocular images extracted from portrait pictures downloaded from websites and social media present relevant differences and additional non-idealities with respect to the samples pertaining to the current databases of ocular images. In fact, the procedure used to capture portrait pictures posted on websites and social media cannot be controlled to maximize the quality of the biometric samples. These pictures are captured using heterogeneous cameras, with different focal lengths, and at diverse distances from the sensor. Furthermore, the illumination conditions can be non-ideal and the users are frequently uncooperative.

To fill this gap and point the research community to the possibility of performing a high-accuracy iris recognition, this paper presents I-SOCIAL-DB[1], the first database of ocular images collected from portrait pictures downloaded from websites and social media. This database is designed for evaluating the performance of iris segmentation and recognition methods in this challenging scenario. For each ocular image, I-SOCIAL-DB includes a segmentation mask created by a human expert and representing the iris contours, occlusions, and reflections. To simplify the use of the manually segmented masks in conjunction with state-of-the-art feature extraction and matching methods, for each ocular image, I-SOCIAL-DB includes a text file representing the coordinates of two circles approximating the inner and outer iris boundaries. Fig. 1 shows an example of the files included in I-SOCIAL-DB. Fig. 2 shows examples of ocular images included in I-SOCIAL-DB.

In this paper, we also present a qualitative analysis of the images based on statistical figures of merit, propose evaluation protocols to be adopted for easily comparing the performance of different methods in a uniform manner, and present

benchmark results achieved by applying publicly available software libraries. The performed analyses confirmed the feasibility of using ocular images collected from websites and social media for iris recognition. We hope that this initiative can give a new challenging public dataset and a new test tool to the academic and industrial research communities working in image processing, pattern recognition, and biometrics, aiming to stimulate new studies in this important field of research.

The paper is organized as follows. Section 2 introduces related works in the literature. Section 3 describes the characteristics of I-SOCIAL-DB. Section 4 presents the results obtained by applying publicly available software libraries for the proposed biometric database. Finally, Section 5 concludes the work.

2. Related Work

The goal of the first studies on biometric systems based on images collected from websites and social media was to design face recognition techniques for searching and tagging users in web-based applications [37]. Recent advances in machine learning enabled the realization of face recognition systems with significantly better performance and robustness [21]. However, methods based on machine learning are trained using datasets composed of huge numbers of images, which could be too much time consuming and expensive to collect using a dedicated acquisition procedure. Therefore, the use of datasets of images collected from websites and social media has become a common practice to train face recognition systems. An example of public dataset composed of face samples collected from public websites is CASIA-WebFace [59], which includes $500,000$ images with labeled identity, collected from $10,000$ subjects using the IMDb website. A more recent example is VGGFace2 [4], composed of 3.31 million images with labeled identity of $9,131$ subjects, obtained using Google Image Search. An example of dataset presenting additional annotations with respect to the identity labels is Density in Face [35], composed of 1 million samples collected from Flickr and including annotations of the craniofacial distances, areas and ratios, facial symmetry and contrast, skin color, age and gender, subjective annotations, pose, and resolution.

Despite the availability of several face recognition datasets collected from public websites, the current datasets are designed for training biometric recognition systems based only on the face. As a consequence, they are composed of images with resolution insufficient for extracting ocular regions in which the iris has a sufficient diameter to be processed using state-of-the-art iris recognition methods.

Currently, to develop algorithms for processing the iris and performing a biometric recognition, it is necessary to consider ad-hoc ocular datasets depicting the iris region with sufficient resolution. It is possible to divide these datasets in two types, according to the type of illumination used: *i)* datasets captured in near-infrared illumination, and *ii)* datasets captured in visible light conditions. The first class includes several publicly available iris datasets collected using com-

---

[1]http://iebil.di.unimi.it/ISocialDB/index.html
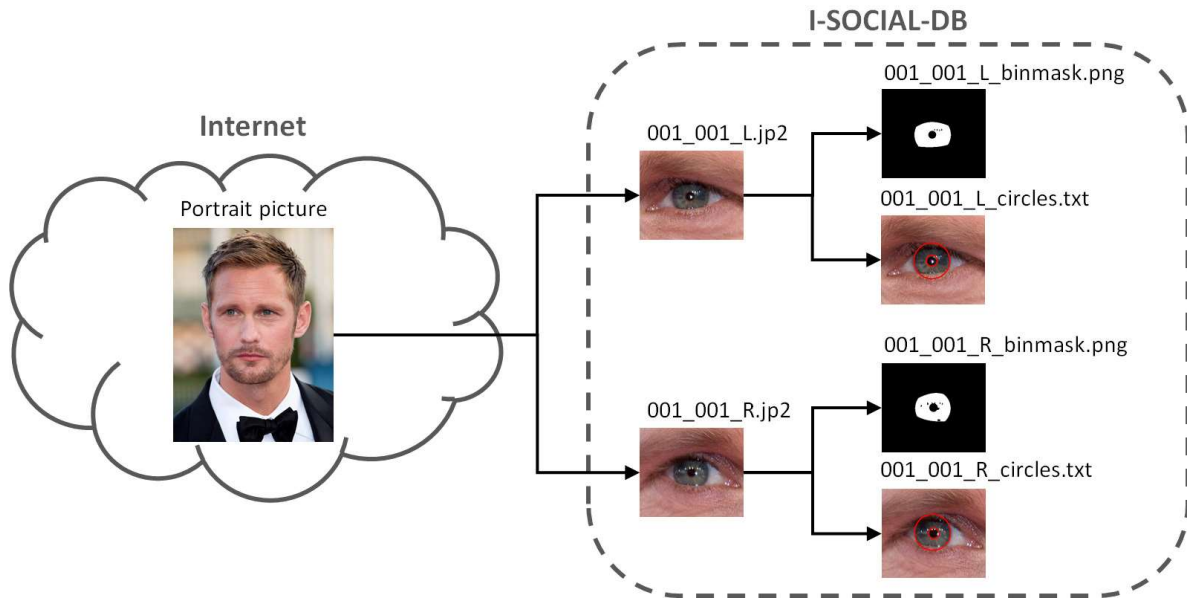
Figure 1: Schema of the file structures included in I-SOCIAL-DB. From a portrait picture downloaded from the web, we extracted and included in I-SOCIAL-DB the following files: two images representing the ocular regions, the pixelwise iris segmentation masks created by a human operator, and textual files describing the parameters of the circles approximating the inner and outer iris boundaries (as an example, in this figure the portrait is assumed to be the sample n. 1 of individual n. 1).
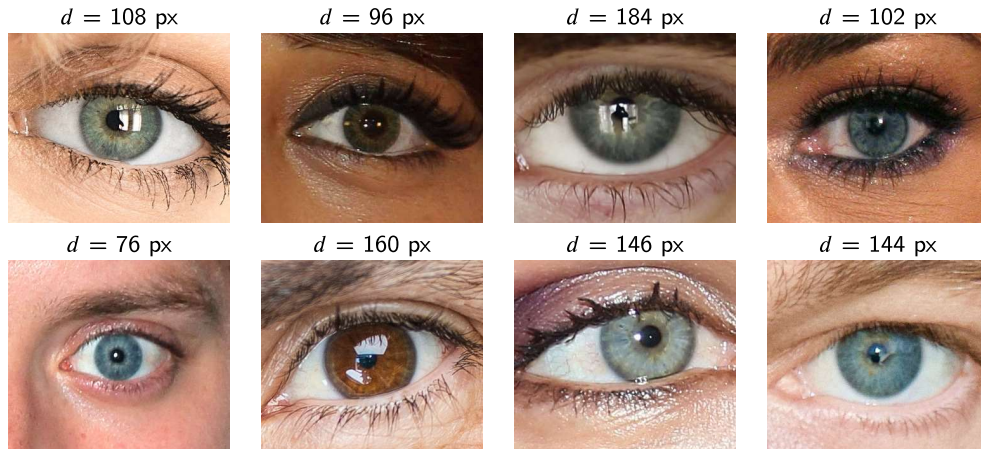
Figure 2: Examples of ocular images of I-SOCIAL-DB, collected from websites and social media, along with the corresponding iris diameter d. The iris diameter is sufficient to perform iris recognition using recent state-of-the-art algorithms.

mercial iris scanners and composed of ocular images from cooperative users [29, 56] or using low-quality samples acquired using iris scanners with the purpose of designing recognition approaches robust to non-ideal acquisitions [5, 39]. There are also datasets of samples acquired from less-cooperative individuals using digital cameras placed at a distance of few meters from the subject and adopting near-infrared illumination techniques to enhance the visibility of the iris pattern [26, 41, 56]. The second class of datasets mostly include image archives composed of samples with reduced visibility of the iris pattern and acquired in visible light conditions from cooperative individuals by using smartphones and

tablets [13, 49, 54]. In addition, the dataset of ocular images UBIRIS v2 [43] has been collected using a less-constrained acquisition procedure and is composed of samples acquired using a digital camera placed at a distance of few meters from the subject, in visible light conditions, and while the user is walking.

All the datasets of ocular images publicly available have been collected using dedicated acquisition procedures. Currently, there are no public datasets of ocular images collected from the web. To fill this gap, we introduce I-SOCIAL-DB, which contains images of ocular regions collected from public websites and social media. The images composing

Table 1
Comparison between I-SOCIAL-DB and public datasets of ocular images acquired in less constrained conditions.

Dataset	Samples Images	Individuals	Illumination	Acquisition Device	Distance	User Cooperation	Segm. Masks
UBIRIS v1 [41]	1,877 single eye images	241	Near infrared, single setting	Nikon E5700	Constant, 20 cm	The user looks to the camera	No
CASIA [56] Iris-Distance	2,567 dual eyes images	142	Near infrared, single setting	Self-realized acquisition system	Constant 3 m	The user looks to the camera	No
QFIRE [26]	10,530 dual eyes videos	195	Near infrared, 3 settings	Dalsa 4M30	Inconstant, from 5 ft to 25 ft	The user walks looking to the camera	No
MobBio [54]	800 single eye images	100	Visible light, 2 settings	Asus Eee Pad Transformer TE300T Tablet	Constant, close to the camera	Cooperative users	Yes [1]
VISOB [49]	158,136 single eye images	550	Visible light, multiple settings	3 smartphones (anterior camera)	Constant, close to the camera	The user captures a selfie image	No
MICHE [13]	3,732 single eye images	92	Visible light, uncontrolled	3 smartphones (anterior and posterior cameras)	Inconstant, close to the camera	Cooperative users	Partially [13]
UBIRIS v2 [43]	11,102 single eye images	261	Visible light, single setting	Canon Eos 5D	Inconstant, from 3 m to 10 m	The user walks looking to the camera	Partially [22, 40]
I-SOCIAL-DB	**3,286 single eye images ***	**400 ****	**Visible light, uncontrolled**	**Heterogeneous, unknown**	**Inconstant, unknown**	**Uncooperative users**	**Yes**

Notes: * 1643 left eye images + 1643 right eye images; ** 800 eyes.

I-SOCIAL-DB are more challenging and closer to that of completely uncontrolled and unconstrained application conditions with respect to the ones of the other publicly available datasets, since the users are not cooperative and the images have been acquired in visible light with unknown conditions, such as the acquisition devices, environmental light conditions, and distances between the eyes and the cameras. Table 1 presents a comparison between I-SOCIAL-DB and the other public datasets of ocular images acquired in less-constrained conditions.

3. Dataset Description

This section describes the proposed I-SOCIAL-DB dataset, with particular focus on the collection procedure, dataset content, non-idealities, and statistical analysis of the biometric features.

3.1. Collection Procedure

To create I-SOCIAL-DB, we collected a set of $1,643$ portrait images from 400 individuals by using Google Image Search and querying for high-resolution images. To obtain images with labeled identities, we searched for famous artists, athletes, and public persons. We balanced the percentage of males and females, obtaining samples from 43.75% males and 56.25% females.

During the collection of the dataset samples, we focused on representing the widest range possible of the different colors of the eyes. For this reason, most of the images have been collected from Caucasian individuals (95.25% of the samples). According to classification proposed in [43], we performed a visual inspection of the samples, observing that 46.5% of the eyes are "Light" pigmented, 37.5% are "Medium" pigmented, and 16.0% are "Heavy" pigmented.

The real ages of the individuals are unknown. Therefore, we estimated the age distribution of the samples by using a method based on convolutional neural networks and feedforward neural networks, described in [2]. We trained the neural networks of the method presented in [2] using the AgeDB database [36]. To estimate the age for each individual, we applied the trained neural networks to each face image from which we obtained the ocular images of I-SOCIAL-DB. We obtained an average age of 44.5 years, with a standard deviation of 10.5 years. The minimum and maximum estimated age are 19 and 84 years, respectively. Fig. 3 shows the estimated age distribution.
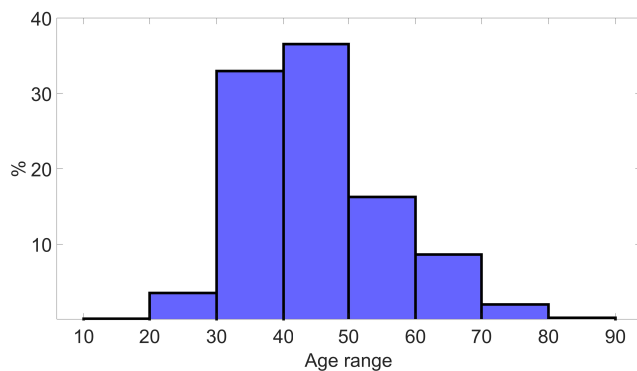
Figure 3: Distribution of the estimated ages of I-SOCIAL-DB, obtained by applying the method based on deep learning [2] on the face images.

3.2. Dataset Content

From every high-resolution face image collected from the web, we cropped the left and right iris regions as rectangles of 350 by 300 pixels centered around the eye coordinates, estimated using a publicly available face detection software [60]. The left and right iris images are saved in JPEG 2000 format, due to its capability of reducing the file size while preserving the visibility of the discriminative details of the iris pattern [10]. Every file name is composed of three digits representing the identifier of the subject, the underscore symbol, three digits representing the number of sample, followed by the character "L" or "R" for the left and right eye respectively (e.g., 001_001_L.jp2 and 001_001-_R.jp2).

From every ocular image, a human expert extracted a binary mask representing the iris region. Similarly to [1], we considered the inner and outer iris boundaries as two non-concentric circles and approximated the eyelids and eyelashes using polynomial curves. In addition, we refined the segmentation masks by segmenting pixelwise possible reflections. We saved the segmentation masks in the uncompressed PNG format. For each iris sample, the name of the corresponding binary image is composed of the one of the ocular image followed by the string "binmask" (e.g., the segmentation mask of the ocular image 001_001_L.jp2 is 001_001-_L_binmask.png).

For every ocular image, I-SOCIAL-DB also includes a textual file reporting the center coordinates and radii of the circles approximating the inner and outer iris boundaries. Specifically, each file includes: x coordinate of the center of the inner boundary, y coordinate of the center of the inner boundary, radius of the circle approximating the inner boundary, x coordinate of the center of the outer boundary, y coordinate of the center of the outer boundary, radius of the circle approximating the outer boundary. For each iris sample, we created a space separated text file with name composed of the one of the corresponding ocular image followed by the string "circles" (e.g., the file corresponding to the ocular image 001_001_L.jp2 is 001_001_L_circles.txt).

Fig. 1 shows an example of files stored in I-SOCIAL-DB for a portrait image collected from the web.

For each collected face image, the database contains two images representing the ocular regions, the pixelwise iris segmentation masks created by a human operator, and textual files describing the parameters of the circles approximating the inner and outer iris boundaries. However, we did not include the face images to preserve the privacy of the individuals [11]. In fact, identifying the name of the owner of the biometric data in the web by only using ocular images is an extremely challenging task for human observers as well as for the current iris recognition algorithms. Differently, face images of famous people can be easily recognized by human observers.

3.3. Non-idealities

Ocular images obtained from the web are visible wavelength images typically acquired by the users or photographers with a visual quality comparable to that of images acquired using mobile devices for selfie-based recognitions [13, 49, 54] and to that of ocular images acquired in natural light conditions, at a distance of some meters from the acquisition sensor and on the move [43]. However, the images of I-SOCIAL-DB present the following additional non-idealities.

- The illumination is uncontrolled and could be related to heterogeneous sources of light. Therefore, the mean intensity of the iris texture, the iris-sclera contrast, and the iris-pupil contrast could be insufficient and non-uniform in different regions of the same sample.

- The images contain strong differences caused by heterogeneous environmental light conditions and illumination techniques. This problem is more relevant with respect to acquisition setups adopting techniques for controlling the illumination.

- The iris and pupil regions could present stronger and larger reflections with respect to the ones present in samples acquired in controlled conditions. As an example, the images can present reflections coming from windows and indoor lights or created by illumination techniques adopted by fashion photographers (which can have different shapes, like a ring or hexagon).

- The images have been acquired using different cameras and lenses, thus including heterogeneous types of distortions and optical aberrations. For the other datasets of ocular images present in the literature, this problem is less relevant since those datasets are composed of images acquired using a limited set of devices.

- The image resolution is non-constant and unknown since there is no available information on the camera model and placement. Therefore, feature extraction and matching methods should be particularly robust to different image sizes.

- The images can present high levels of sensor noise, typically introduced in case of acquisitions performed

in low light conditions. This problem is more relevant with respect to the other publicly available datasets of ocular images, acquired in more controlled illumination conditions.

- The eyelids and eyelashes frequently present strong make up, which could significantly reduce the accuracy of the segmentation algorithms [19]. This problem is more frequent and relevant with respect to ocular images collected in universities and research institutes since people tend to use less make up in working environments with respect to special events or photographic sessions for which people decide to upload their portraits to websites and social media.

- The images could have been postprocessed by the subjects to enhance their visual aspect before uploading their pictures on websites or social media. As a consequence, the iris texture can be more frequently blurred with respect to samples specifically collected to evaluate biometric recognition algorithms. These image modifications could negatively affect the accuracy of iris segmentation and recognition methods.

3.4. Statistical Analysis of the Biometric Features and Image Quality

To estimate the quality of the ocular images, we performed an evaluation of some of the features that influence the most the accuracy of iris recognition systems [53, 55].

Iris diameter. It is frequently used to describe the resolution of the iris region and is relevant to evaluate the amount of discriminant information that can be extracted by iris recognition methods. For the proposed dataset I-SOCIAL-DB, we estimated a mean iris diameter of 112.1 pixels, with a standard deviation of 28.3 pixels. The minimum and maximum values are 44.8 and 274.0 pixels, respectively. For traditional iris recognition systems, the diameter values should usually be close to 140 pixels, as suggested in [7]. Nevertheless, recent studies proved the possibility of achieving relevant accuracy using iris images of lower resolution [50].

Usable iris area. It represents the portion of the iris area usable for biometric recognition and not covered by occlusions and reflections. We considered the total iris area a as the ring included in the circles approximating the inner and outer iris boundaries and the usable area a' as the area described by the segmentation mask created by a human expert. The usable iris area has been computed as a'/a. For the proposed dataset, we obtained a mean usable area of 71.4%, with a standard deviation of 11.9%. The minimum and maximum values are 33.4% and 100.0%, respectively. According to [7], the percentage of usable iris area acceptable for biometric recognition should be greater than 50%.

Dilation. It describes the changes of the pupil size due to the illumination conditions. Studies in the literature [23] proved that identity comparisons between images describing dilated and close pupils can obtain poor accuracy. We computed this parameter as the ratio between the outer and inner iris radius.

For the proposed dataset, we obtained a mean ratio of 27.1%, with a standard deviation of 6.3%. The minimum and maximum values are 9.6% and 57.1%, respectively. These values highlight the need of using recognition algorithms robust to heterogeneous values of pupil dilation.

Pupil-iris contrast. It describes the intensity difference between the pupil and iris regions. A low pupil-iris contrast can negatively affect the accuracy of iris segmentation algorithms [55]. Since many methods in the literature consider the red channel as the most discriminating channel for ocular iris images acquired in visible light conditions [16, 40], we computed the pupil-iris contrast from the red channel R of the ocular image I. This parameter has been computed as the median of R in the region of interest described by the segmentation mask minus the median of R in the circle representing the pupil region. For the proposed dataset, we obtained a mean pupil-iris contrast of 34.4, with a standard deviation of 23.4. The minimum and maximum values are 0 and 142, respectively. The iris boundary is visible for human observers even in the cases in which this feature is equal to 0 since the pupil-iris contrast has been computed considering the median intensity of local image regions of the red channel. However, the obtained mean value suggests the need of segmentation algorithms robust to low contrast between the pupil and iris regions.

Iris-sclera contrast. It describes the intensity difference between the iris and sclera regions. A low iris-sclera contrast can negatively affect the accuracy of iris segmentation algorithms [55]. We estimated the iris-sclera contrast for the red channel R of the ocular image I. This parameter has been computed as the the median of R in a region of the sclera manually selected by a human expert minus the median of R in the region of interest described by the segmentation mask. For the proposed dataset, we obtained a mean iris-sclera contrast of 97.1, with a standard deviation of 37.4. The minimum and maximum values are 0 and 218, respectively. The iris boundary is visible for human observers even in the cases in which this feature is equal to 0 since the iris-sclera contrast has been computed considering the median intensity of local image regions of the red channel. However, the obtained standard deviation suggests the need of segmentation algorithms particularly robust to heterogeneous contrast conditions.

Iris contrast. It provides information related to the eye color and illumination conditions. The discriminating details of the iris pattern are usually difficult to distinguish in low-contrast images. We estimated the iris contrast considering the region described by the segmentation mask of the red channel R of the ocular image I. The contrast has been computed as the difference between the maximum and minimum intensity of the region. For the proposed dataset, we obtained a mean iris contrast of 187.2, with a standard deviation of 44.7. The minimum and maximum values are 28 and 255, respectively. The standard deviation value shows that the images present relevant differences in terms of visibility of the iris pattern.

Table 2

Summary of the biometric features and quality measures defined in Subsection 3.4 for I-SOCIAL-DB.

I-SOCIAL-DB	Value		
Number of images	3286 ocular images		
Number of individuals	400 (800 different eyes)		
Image size (px)	300×350		

Feature	Mean	Std	Min	Max
Number of images / eye	4.1	2.1	2	6
Iris diameter (px)	112.1	28.3	44.8	274.0
Usable iris area (%)	71.4	11.9	33.4	100.0
Dilation (%)	27.1	6.3	9.6	57.1
Pupil-iris contrast (red channel)	34.4	23.4	0	142
Iris-sclera contrast (red channel)	97.1	37.4	0	218
Iris contrast (red channel)	187.2	44.7	28	255
Iris sharpness (red channel)	6.7	2.7	1.3	28.4
Iris intensity (red channel)	63.3	27.9	3.1	156.2

Iris sharpness. It provides information on the amount of distinctive details of the iris pattern visible in the ocular image. We computed the iris sharpness for the region described by the segmentation mask of the red channel R of the ocular image I. We computed the sharpness parameter as the sum of the gradient magnitude normalized according to the number of pixels n. For the proposed dataset, we obtained a mean sharpness of 6.7, with a standard deviation of 2.7. The minimum and maximum values are 1.3 and 28.4, respectively. Compared to the mean value, the obtained standard deviation shows a high variability of the iris sharpness in the images of the dataset, thus proving the need of feature extraction algorithms robust to heterogeneous levels of visibility of the iris texture.

Iris intensity. It provides information on the eye color and illumination conditions. High intensity images usually correspond to eyes of light color, in which the details of the iris texture are easily distinguishable in visible light conditions. We computed the iris intensity for the region described by the segmentation mask of the red channel R of the ocular image I. For the proposed dataset, we obtained a mean iris intensity of 63.3, with a standard deviation of 27.9. The minimum and maximum values are 3.1 and 156.2, respectively. The standard deviation value indicates the presence of eyes of different colors.

Fig. 4 shows the boxplots of the biometric features estimated for the ocular images of I-SOCIAL-DB. The graphs show that the images present a high variability in acquisition conditions and level of visible details, thus representing a challenging but useful tool for designing biometric methods robust to acquisitions performed in unconstrained, uncontrolled, and uncooperative conditions.

Table 2 summarizes the biometric features and quality measures of the images in the dataset considered in this paper, according to the definitions given in Section 3.4.

4. Benchmark Results

This section presents the results of performance evaluations of iris-based biometric algorithms for I-SOCIAL-DB. In particular, we describe the evaluation protocol, present the segmentation accuracy of public software libraries, and report the identity verification accuracy of publicly available methods.

4.1. Evaluation Protocol

The proposed dataset is principally designed as a testbed for monomodal iris recognition approaches, but it can also be used to design and evaluate multibiometric recognition approaches based on the fusion of two iris textures. Moreover, I-SOCIAL-DB allows to evaluate the accuracy of iris segmentation as well as biometric recognition approaches.

To evaluate the accuracy of segmentation approaches, we used the segmentation masks included in I-SOCIAL-DB to perform a pixelwise accuracy assessment. To this purpose, we considered two figures of merit commonly used in the literature, introduced for the competition NICE.I [42]. The first metric (E1) represents the classification error rate and is computed as the proportion of disagreeing pixels between each computed segmentation mask O and the corresponding ground truth mask C, as follows:

$$E1 = \frac{1}{n} \sum_i \frac{1}{c \times r} \sum_{c'} \sum_{r'} O_i(c', r') \otimes C_i(c', r') \ , \quad (1)$$

where n is the number of ocular images, c is the column index, r is the row index, and $\otimes$ represents the XOR operation. The second metric (E2) considers the False Positive Rate (FPR) and False Negative Rate (FNR) of the pixel classification, and is computed as follows:

$$E2 = (1/n) \times 0.5 \times FPR_i + 0.5 \times FNR_i \ . \quad (2)$$

To evaluate the accuracy of biometric recognition approaches, we performed a technology evaluation [25] to compare the performance of different state-of-the-art methods.
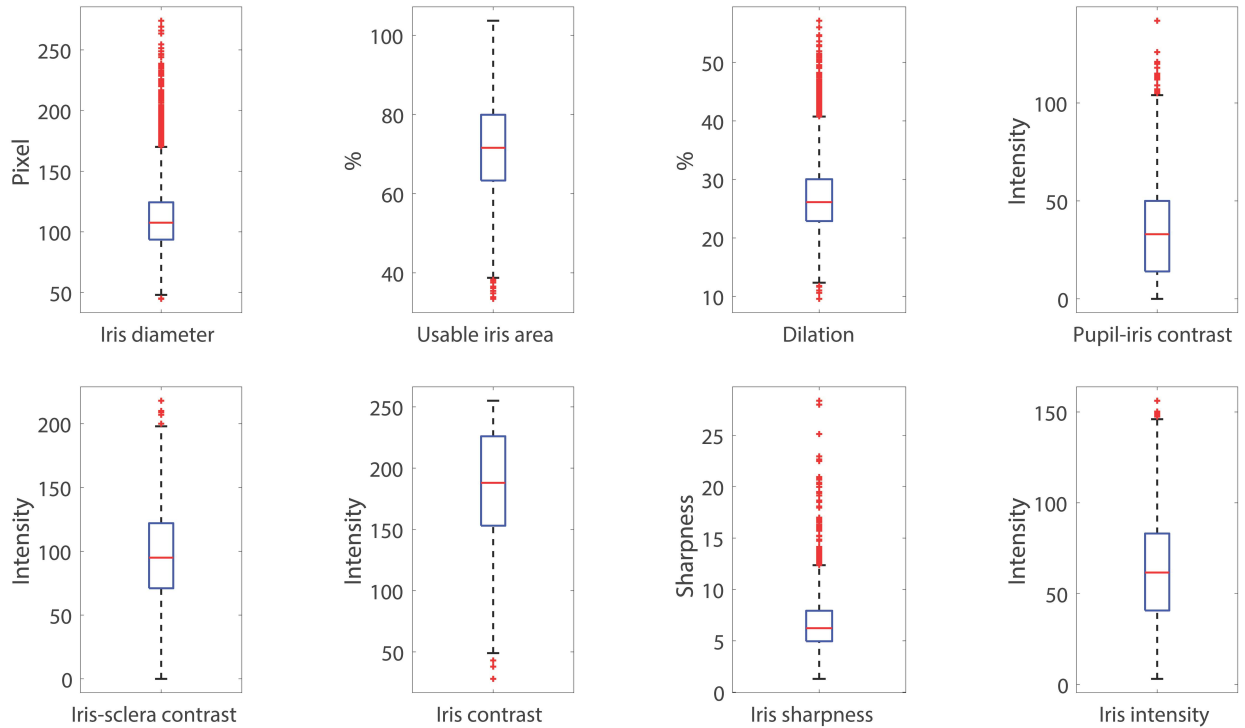
Figure 4: Boxplots obtained for the biometric features estimated for the ocular images of I-SOCIAL-DB.

As figures of merit we considered the Equal Error Rate (EER) [24] and the False Match Rate (FMR) corresponding to False Non Match Rate (FNMR) of 1% [31].

4.2. Segmentation Accuracy

To provide a first benchmark for future research work, we evaluated the segmentation accuracy obtained on I-SO-CIAL-DB using publicly available software libraries for iris segmentation. In particular, we considered a segmentation method based on the Total Variation Model (Tvm) [61], the algorithm included in Osiris version 4.1 (Osiris) [38], a fast segmentation algorithm for non-ideal images (Fsa) [20], a segmentation technique based on deep learning (Deep) [27], and three segmentation algorithms included in USIT version 2.2 [46]: Contrast-Adjusted Hough Transform (Caht) [45], Iterative Fourier-series Push and Pull (Ifpp) [8], and Weighted Adaptive Hough and Ellipsopolar Transform (Wahet) [57].

To provide a comparison with other public datasets, we analyzed the results obtained by the considered software libraries for I-SOCIAL-DB and for the following sets of ocular images.

- *DB UBIRIS v2*, a dataset of ocular images acquired in natural light conditions, from walking individuals, at different distances from the camera, and in natural light conditions. Specifically, DB UBIRIS v2 consists of a subset of 2,250 samples of UBIRIS v2 [43] for which manually segmented masks are publicly available [22]. We used as ground truth the masks created by Operator A [22].

- *DB IITD*, a dataset of ocular imaged acquired using commercial iris scanners in controlled conditions. Specifically, DB IITD is a subset of 1,120 samples of the "IIT Delhi Iris Database Version 1.0" database [29] for which manually segmented masks are publicly available [22]. We used as ground truth the masks created by Operator A [22].

Table 3 summarizes the obtained results. The results should be considered as examples of the performance obtainable by current state-of-the-art techniques, considering that the we only modified the parameters describing the minimum and maximum radii approximating the iris boundaries, without fine tuning any other parameters.

The segmentation method that obtained the best performance for I-SOCIAL-DB is Deep, which accurately estimated the external iris boundaries for most of the samples. However, it failed to extract the pupil-iris boundary for many ocular images. Although the best accuracy obtained by most of the evaluated methods is inferior to that obtained for other datasets of ocular images, these results can be considered as encouraging since they have been obtained without performing any tuning of the segmentation methods for this kind of challenging images.

4.3. Identity Verification Accuracy

We evaluated the identity verification accuracy obtained using publicly available iris recognition methods applied on I-SOCIAL-DB and using the provided segmentation masks created by a human expert. In particular, we evaluated the recognition method included in Osiris version 4.1 (OSIRIS)

Table 3

Pixelwise iris segmentation accuracy using publicly available segmentation libraries for I-SOCIAL-DB and two reference public datasets.

Segmentation Library	I-SOCIAL-DB Segmentation error		UBIRIS Segmentation Error		IITD Segmentation Error	
	E1	E2	E1	E2	E1	E2
Wahet [57]	0.1347	0.2831	0.2621	0.4783	0.0978	0.0951
Ifpp [8]	0.1121	0.1855	0.2282	0.3789	0.0911	0.0831
Fsa [20]	0.0943	0.3226	0.1720	0.4310	0.0330	0.0364
Caht [45]	0.0862	0.4042	0.1088	0.4525	0.0494	0.0695
Osiris [38]	0.0540	0.3556	0.1069	0.3816	0.0477	0.0504
Tvm [61]	0.0316	0.1406	0.0211	0.1172	0.3422	0.5048
Deep [27]	0.0214	0.0614	0.0228	0.0978	0.0281	0.0363

Table 4

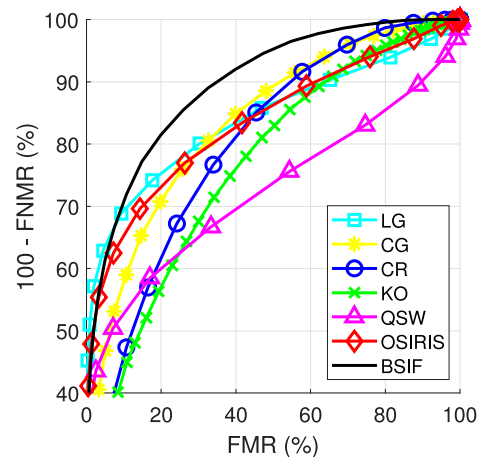Identity verification accuracy using publicly available iris recognition libraries for I-SOCIAL-DB.

| Iris Recognition Library	EER (%)	FMR @ FNMR = 1% (%)
QSW [30]	32.75	60.93
KO [28]	31.26	84.80
CR [44]	28.36	83.47
CG [7]	24.82	74.07
OSIRIS [38]	23.96	53.54
LG [32]	22.70	47.18
BSIF [6]	18.97	56.33

Figure 5: ROC curves obtained by different feature extraction and matching algorithms for the images and manually segmented masks of I-SOCIAL-DB. Although the error obtained for I-SOCIAL-DB is higher with respect to the one obtained for datasets collected in more controlled and cooperative conditions, the obtained results confirm the feasibility of applying iris recognition techniques to high-resolution portrait pictures uploaded on websites and social media.

[38], a method based on machine learning called Binarized Statistical Image Features (BSIF) [6], and the following recognition methods implemented in USIT version 2.2 [46]: Log Gabor (LG) [32], Complex Gabor (CG) [7], Local intensity variations (CR) [44], Cumulative sums of gray scale blocks (KO) [28], Quadratic Spline Wavelet (QSW) [30].

Table 4 summarizes the obtained results, while Fig. 5 shows the obtained ROC curves. The results should be considered as examples of the performance obtainable by current state-of-the-art techniques, considering that the we did not fine tune their parameters for I-SOCIAL-DB and small differences in the computational chain could imply variations in terms of the overall recognition accuracy.

BSIF achieved the best EER (18.97%) and the best accuracy for most of the regions of the ROC curve, while LG achieved the best FMR at FNMR equal to 1% (47.18%). Although the error obtained for I-SOCIAL-DB is higher with respect to the one obtained for datasets collected in more controlled and cooperative conditions [14, 16], the obtained results confirm the feasibility of applying iris recognition techniques to high-resolution portrait pictures uploaded on websites and social media.

As an example, Fig. 6 shows the distribution of the genuine and impostor matching scores obtained for I-SOCIAL-DB using the provided segmentation masks and the biometric recognition schema LG [32]. It is possible to observe that many genuine matching scores have values comparable to the ones obtained by the same biometric recognition approach for ocular images acquired using traditional iris scanners.

To compare the recognition accuracy of state of state-of-the-art methods for I-SOCIAL-DB and other datasets of ocular images, we also perfomed identity verification tests by combining the segmentation methods used to compute Table 3 with the identity verification algorithm LG [32]. We obtained the best accuracy using the segmentation algorithm Tvm [61], achieving an EER = 35.60%. This result is similar to that obtained by the same algorithms for ocular images acquired in visible light, like the ones of UBIRIS v2 [16].

5. Conclusion

This paper introduced I-SOCIAL-DB, the first biometric dataset of ocular images collected from public websites
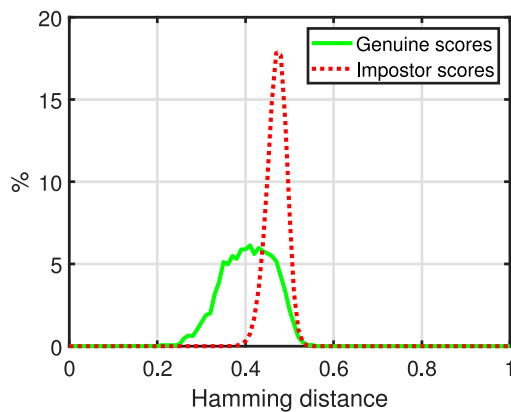
Figure 6: Distribution of the genuine and impostor matching scores obtained for I-SOCIAL-DB using iris segmentation masks created by a human expert and the biometric recognition method Log Gabor (LG) [32]. Many genuine matching scores have values comparable to the ones obtained by the same biometric recognition approach for ocular images acquired using traditional iris scanners.

and social media. I-SOCIAL-DB includes $3,286$ single eye images, obtained from $1,643$ face images of 400 individuals (800 different eyes, for a total of $1,643$ images of left eyes and $1,643$ images of right eyes). For each ocular image, the dataset includes the corresponding iris segmentation masks created by a human expert, and the parameters describing the circles approximating the inner and outer iris boundaries. The segmentation masks describe pixelwise the iris contours, reflections, and occlusions.

To provide detailed information on I-SOCIAL-DB, this paper presented the results of a statistical analysis of the biometric features of the ocular images. Furthermore, this paper provided benchmark results for I-SOCIAL-DB, obtained by applying public software libraries for iris segmentation and recognition. The performed tests proved the feasibility of using images collected from the web for iris recognition.

We hope that I-SOCIAL-DB can help the research and industrial communities working in biometrics, image processing, and pattern recognition to further improve the current algorithms, systems, and technologies for iris recognition in uncontrolled environments.

Future works can consider expanding the dataset by considering a more balanced distribution of the ethnicities and analyzing the effect of race bias on iris recognition.

6. Acknowledgments

References

[1] Alonso-Fernandez, F., Bigün, J., 2015. Near-infrared and visible-light periocular recognition with gabor features using frequency-adaptive automatic eye detection. IET Biometrics 4, 74–89.

[2] Anand, A., Donida Labati, R., Genovese, A., Muñoz, E., Piuri, V., Scotti, F., 2017. Age estimation based on face images and pre-trained Convolutional Neural Networks, in: Proc. of the 2017 IEEE Symp. on Computational Intelligence for Security and Defense Applications (CISDA), pp. 1–7.

[3] Bowyer, K.W., 2012. The results of the NICE.II iris biometrics competition. Pattern Recognition Letters 33, 965–969.

[4] Cao, Q., Shen, L., Xie, W., Parkhi, O.M., Zisserman, A., 2018. VGGFace2: A dataset for recognising faces across pose and age, in: Proc. of the 13th IEEE Int. Conf. on Automatic Face Gesture Recognition (FG), pp. 67–74.

[5] Crihalmeanu, S., Ross, A., Schuckers, S., Hornak, L., 2007. A Protocol for Multibiometric Data Acquisition, Storage and Dissemination. Technical Report. Lane Depart. Comput. Sci. and Elect. Eng., West Virginia University.

[6] Czajka, A., Moreira, D., Bowyer, K., Flynn, P., 2019. Domain-specific human-inspired binarized statistical image features for iris recognition, in: Proc. of the IEEE Winter Conf. on Applications of Computer Vision (WACV), pp. 959–967.

[7] Daugman, J., 2004. How iris recognition works. IEEE Trans. on Circuits and Systems for Video Technology 14, 21–30.

[8] Daugman, J., 2007. New methods in iris recognition. IEEE Trans. on Systems, Man, and Cybernetics, Part B (Cybernetics) 37, 1167–1175.

[9] Daugman, J., 2016. Information theory and the IrisCode. IEEE Trans. on Information Forensics and Security 11, 400–409.

[10] Daugman, J., Downing, C., 2008. Effect of severe image compression on iris recognition performance. IEEE Trans. on Information Forensics and Security 3, 52–61.

[11] De Capitani di Vimercati, S., Foresti, S., Livraga, G., Samarati, P., 2012. Data privacy: Definitions and techniques. International Journal of Uncertainty, Fuzziness and Knowledge-Based Systems 20, 793–817.

[12] De Marsico, M., Nappi, M., Proença, H., 2017. Results from MICHE II – Mobile Iris CHallenge Evaluation II. Pattern Recognition Letters 91, 3–10.

[13] De Marsico, M., Nappi, M., Riccio, D., Wechsler, H., 2015. Mobile Iris Challenge Evaluation (MICHE)-I, biometric iris dataset and protocols. Pattern Recognition Letters 57, 17–23.

[14] Donida Labati, R., Genovese, A., Piuri, V., Scotti, F., 2012. Iris segmentation: state of the art and innovative methods, in: Liu, C., Mago, V. (Eds.), Cross Disciplinary Biometric Systems. Springer Berlin Heidelberg. volume 37 of *Intelligent Systems Reference Library*, pp. 151–182.

[15] Donida Labati, R., Genovese, A., Piuri, V., Scotti, F., 2019a. A scheme for fingerphoto recognition in smartphones, in: Rattani, A., Derakhshani, R., Ross, A. (Eds.), Selfie Biometrics. Springer, Cham. Advances in Computer Vision and Pattern Recognition, pp. 49–66.

[16] Donida Labati, R., Muñoz, E., Piuri, V., Ross, A., Scotti, F., 2019b. Non-ideal iris segmentation using Polar Spline RANSAC and illumination compensation. Computer Vision and Image Understanding 188, 102787.

[17] Donida Labati, R., Piuri, V., Scotti, F., 2009. Agent-based image iris segmentation and multiple views boundary refining, in: Proc. of the 2009 IEEE Int. Conf. on Biometrics: Theory, Applications and Systems (BTAS), pp. 1–7.

[18] Donida Labati, R., Scotti, F., 2010. Noisy iris segmentation with boundary regularization and reflections removal. Image and Vision Computing, Iris Images Segmentation Special Issue 28, 270–277.

[19] Doyle, J.S., Flynn, P.J., Bowyer, K.W., 2013. Effects of mascara on iris recognition, in: Biometric and Surveillance Technology for Human and Activity Identification X, International Society for Optics and Photonics. pp. 126–136.

[20] Gangwar, A., Joshi, A., Singh, A., Alonso-Fernandez, F., Bigun, J., 2016. IrisSeg: A fast and robust iris segmentation framework for non-ideal iris images, in: Proc. of the Int. Conf. on Biometrics, pp. 1–8.

[21] Guo, G., Zhang, N., 2019. A survey on deep learning based face recognition. Computer Vision and Image Understanding 189, 102805.

[22] Hofbauer, H., Alonso-Fernandez, F., Wild, P., Bigün, J., Uhl, A., 2014. A ground truth for iris segmentation, in: Proc. of the 2014 22nd Int. Conf. on Pattern Recognition (ICPR), pp. 527–532.

[23] Hollingsworth, K., Bowyer, K.W., Flynn, P.J., 2009. Pupil dilation degrades iris biometric performance. Compututer Vision and Image Understanding 113, 150–157.

[24] Jain, A.K., Flynn, P., Ross, A.A., 2007. Handbook of Biometrics. Springer-Verlag New York, Inc., Secaucus, NJ, USA.

[25] Jang, J., Kim, H., 2009. Performance measures, in: Li, S., Jain, A. (Eds.), Encyclopedia of Biometrics. Springer, pp. 1062–1068.

[26] Johnson, P., Lopez-Meyer, P., Sazonova, N., Hua, F., Schuckers, S., 2010. Quality in face and iris research ensemble (Q-FIRE), in: Proc. of the 4th IEEE Int. Conf. on Biometrics: Theory, Application and Systems (BTAS), pp. 1–6.

[27] Kerrigan, D., Trokielewicz, M., Czajka, A., Bowyer, K.W., 2019. Iris recognition with image segmentation employing retrained off-the-shelf deep neural networks, in: Proc. of the 12th IAPR Int. Conf. On Biometrics (ICB), pp. 1–7.

[28] Ko, J.G., Gil, Y.H., Yoo, J.H., Chung, K.I., . A novel and efficient feature extraction method for iris recognition. ETRI Journal 29, 399–401.

[29] Kumar, A., Passi, A., 2010. Comparison and combination of iris matchers for reliable personal authentication. Pattern Recognition 43, 1016–1026.

[30] Ma, L., Tan, T., Wang, Y., Zhang, D., 2004. Efficient iris recognition by characterizing key local variations. IEEE Trans. on Image Processing 13, 739–750.

[31] Maio, D., Maltoni, D., Cappelli, R., Wayman, J., Jain, A., 2002. FVC2000: Fingerprint verification competition. IEEE Trans. Pattern Anal. Mach. Intell. 24, 402–412.

[32] Masek, L., Kovesi, P., 2003. MATLAB source code for a biometric identification system based on iris patterns.

[33] Mayhew, S., 2018. DERMALOG iris recognition software matches 25 million eyes per second. https://www.biometricupdate.com/201806/dermalog-iris-recognition-software-matches-25-million-eyes-per-second.

[34] Meng, W., Wong, D.S., Furnell, S., Zhou, J., 2015. Surveying the development of biometric user authentication on mobile phones. IEEE Communications Surveys & Tutorials 17, 1268–1293.

[35] Merler, M., Ratha, N.K., Feris, R.S., Smith, J.R., 2019. Diversity in faces. arXiv .

[36] Moschoglou, S., Papaioannou, A., Sagonas, C., Deng, J., Kotsia, I., Zafeiriou, S., 2017. AgeDB: the first manually collected, in-the-wild age database, in: Proc. of the IEEE Conference on Computer Vision and Pattern Recognition Workshop (CVPRW), pp. 1–5.

[37] Ortiz, E.G., Becker, B.C., 2014. Face recognition for web-scale datasets. Computer Vision and Image Understanding 118, 153–170.

[38] Othman, N., Dorizzi, B., Garcia-Salicetti, S., 2016. OSIRIS: An open source iris recognition software. Pattern Recognition Letters 82, 124–131.

[39] Phillips, P.J., Scruggs, W.T., O'Toole, A.J., Flynn, P.J., Bowyer, K.W., Schott, C.L., Sharpe, M., 2010. FRVT 2006 and ICE 2006 large-scale experimental results. IEEE Trans. on Pattern Analysis and Machine Intelligence 32, 831–846.

[40] Proenca, H., Alexandre, L., 2012a. Toward covert iris biometric recognition: Experimental results from the NICE contests. IEEE Trans. on Information Forensics and Security 7, 798–808.

[41] Proença, H., Alexandre, L.A., 2005. UBIRIS: A noisy iris image database, in: Proc. of the Int. Conf. on Image Analysis and Processing (ICIAP), pp. 970–977.

[42] Proença, H., Alexandre, L.A., 2012b. Introduction to the special issue on the recognition of visible wavelength iris images captured at-a-distance and on-the-move. Pattern Recognition Letters 33, 963–964.

[43] Proença, H., Filipe, S., Santos, R., Oliveira, J., Alexandre, L.A., 2010. The UBIRIS.v2: A database of visible wavelength iris images captured on-the-move and at-a-distance. IEEE Trans. on Pattern Analysis and Machine Intelligence 32, 1529–1535.

[44] Rathgeb, C., Uhl, A., 2010. Secure iris recognition based on local intensity variations, in: Campilho, A., Kamel, M. (Eds.), Proc. of the Int. Conf. on Image Analysis and Recognition (ICIAR), pp. 266–275.

[45] Rathgeb, C., Uhl, A., Wild, P., 2013. Iris Recognition: From Segmentation to Template Security. Springer, Berlin.

[46] Rathgeb, C., Uhl, A., Wild, P., Hofbauer, H., 2016. Design decisions for an iris recognition SDK, in: Bowyer, K.W., Burge, M.J. (Eds.), Handbook of Iris Recognition, Springer London. pp. 359–396.

[47] Rattani, A., Derakhshani, R., 2017. On fine-tuning convolutional neural networks for smartphone based ocular recognition, in: Proc. of the 2017 IEEE Int. Joint Conf. on Biometrics (IJCB), pp. 762–767.

[48] Rattani, A., Derakhshani, R., 2018. A survey of mobile face biometrics. Computers & Electrical Engineering 72, 39–52.

[49] Rattani, A., Derakhshani, R., Saripalle, S.K., Gottemukkula, V., 2016. ICIP 2016 competition on mobile ocular biometric recognition, in: Proc. of the 2016 IEEE Int. Conf. on Image Processing (ICIP), pp. 320–324.

[50] Ribeiro, E., Uhl, A., Alonso-Fernandez, F., 2019. Iris super-resolution using CNNs: is photo-realism important to iris recognition? IET Biometrics 8, 69–78.

[51] Ross, A.A., Nandakumar, K., Jain, A.K., 2006. Handbook of Multi-biometrics (International Series on Biometrics). Springer-Verlag, Berlin, Heidelberg.

[52] Samsung Newsroom, 2019. Samsung takes mobile photography to the next level with industry's first 108mp image sensor for smartphones. https://news.samsung.com/global/samsung-takes-mobile-photography-to-the-next-level-with-industrys-first-108mp-image-sensor-for-smartphones.

[53] Schmid, N.A., Zuo, J., Nicolo, F., Wechsler, H., 2013. Iris quality metrics for adaptive authentication, in: Burge, J.M., Bowyer, W.K. (Eds.), Handbook of Iris Recognition. Springer, London, pp. 67–84.

[54] Sequeira, A.F., Monteiro, J.C., Rebelo, A., Oliveira, H.P., 2014. Mob-BIO: A multimodal database captured with a portable handheld device. Proc. of the 2014 Int. Conf. on Computer Vision Theory and Applications (VISAPP) 3, 133–139.

[55] Tabassi, E., Grother, P., Salamon, W., 2011. Iris Quality Calibration and Evaluation (IQCE): Performance of Iris Image Quality Assessment and Algorithms. Technical Report. Nat. Inst. Standards and Technol. (NIST).

[56] The Center of Biometrics and Security Research, . CASIA-IrisV4. Http://biometrics.idealtest.org.

[57] Wild, P., Hofbauer, H., Ferryman, J., Uhl, A., 2015. Segmentation-level fusion for iris recognition, in: Proc. of the 2015 Int. Conf. of the Biometrics Special Interest Group (BIOSIG), pp. 1–6.

[58] Xiaomi, . Mi Note 10. Https://www.mi.com/global/mi-note-10.

[59] Yi, D., Lei, Z., Liao, S., Li, S.Z., 2014. Learning face representation from scratch. CoRR URL: http://arxiv.org/abs/1411.7923.

[60] Zhang, K., Zhang, Z., Li, Z., Qiao, Y., 2016. Joint face detection and alignment using Multitask Cascaded Convolutional Networks. IEEE Signal Processing Letters 23, 1499–1503.

[61] Zhao, Z., Kumar, A., 2015. An accurate iris segmentation framework under relaxed imaging constraints using total variation model, in: Proc. of the 2015 IEEE Int. Conf. on Computer Vision (ICCV), pp. 3828–3836.